

# Protective Effect of the Human Epineural Patch Application after Sciatic Nerve Crush Injury Followed by Nerve Transection and End-to-End Repair

Maria Siemionow<sup>✉</sup> · Weronika Radecka<sup>✉</sup> · Katarzyna Kozłowska<sup>✉</sup> · Lucile Chambily<sup>✉</sup> · Sonia Brodowska<sup>✉</sup> · Dominika Kuc<sup>✉</sup> · Gabrielle Filipek<sup>✉</sup> · Katarzyna Budzynska<sup>✉</sup>

## Abstract

Nerve regeneration under unfavorable wound conditions remains challenging. We introduce the human epineural patch (hEP) as a novel nerve protector for post-trauma applications, comparing its regenerative efficacy with that of the human amniotic membrane (hAM). Following crush injury, transection, and end-to-end repair (CTR), 36 athymic nude rats were randomly assigned to six experimental groups ( $n = 6$  each): control (no-protection), hEP, or hAM application post-repair. Assessments at 6 weeks and 12 weeks included functional evaluation (Toe-Spread and Pinprick tests), gastrocnemius muscle index (GMI), histomorphometric analysis (myelin thickness, axonal density, fiber diameter, percentage of myelinated fibers), and immunofluorescence staining for neurogenic, angiogenic, and immunogenic markers. The hEP group exhibited superior motor ( $3.167 \pm 0.167$ ) and sensory ( $3.500 \pm 0.212$ ) recovery and GMI values ( $0.955 \pm 0.014$ ), compared with the No protection group ( $p < 0.05$ ). Myelin thickness ( $3.480 \pm 0.019 \mu\text{m}$ ,  $p < 0.0001$ ), fiber diameter ( $10.788 \pm 0.197 \mu\text{m}$ ,  $p < 0.05$ ), and myelinated fiber percentage ( $89.841\% \pm 0.453\%$ ,  $p < 0.01$ ) were significantly higher in the hEP group. At 12 weeks, hEP application significantly increased the expression of Laminin B ( $2.083 \pm 0.083$ ), nerve growth factor (NGF) ( $1.750 \pm 0.250$ ), and vascular endothelial growth factor (VEGF) ( $2.667 \pm 0.333$ ), corresponding with improved function. The application of hEP at the sciatic nerve repair site after CTR injury significantly enhanced nerve regeneration compared with hAM. This study introduces hEP as a promising alternative nerve protector for traumatic nerve injuries.

## Keywords

Peripheral nerve repair • Human epineural patch • Human amniotic membrane • Allografts • Nerve regeneration • Regenerative medicine

Received: 11 January 2025 / Accepted: 25 February 2025/

© L. Hirszfeld Institute of Immunology and Experimental Therapy, Wrocław, Poland 2025

## Abbreviations

AAALAC, American Association for the Accreditation of Laboratory Animal Care; ANOVA, Analysis of Variance; APC, Antigen-Presenting Cell; CTR, crush, transaction, repair; GFAP, glial fibrillary acidic protein; GMI, gastrocnemius muscle index; hAM, human amniotic membrane; hEP, human epineural patch; HLA-DR, human leukocyte antigen-DR; HLA-I, human leukocyte antigen class I; IACUC, Institutional Animal Care and Use Committee; MHC, Major Histocompatibility Complex; MTF, musculoskeletal transplant foundation; NGF, nerve growth factor; S-100, S-100 protein; SEM, standard error of the mean; VEGF, vascular endothelial growth factor; vWF, von Willebrand factor.

## 1. Introduction

Peripheral nerve injuries present a significant clinical challenge, often resulting in substantial functional impairment and long-term disability (Juckett et al. 2022). Despite advancements in microsurgical techniques and novel treatment modalities, many patients fail to achieve complete sensory or motor recovery (Grinsell and Keating 2014; Lopes et al. 2022). The complex nature of peripheral nerve injuries, particularly in unfavorable wound conditions, highlights the urgent

need for innovative strategies to enhance nerve regeneration and prevent adhesions and scar tissue formation around the injury site (Siemionow et al. 2013).

Autologous nerve grafting remains the gold standard for bridging nerve defects when direct repair is not feasible. Alternative clinical approaches, such as acellular nerve grafts and various types of conduits, share common drawbacks, including donor site morbidity, size mismatch, and immunogenicity (Wang et al. 2019; Hussain et al. 2020; Lin and Jain 2023; Meng et al. 2023). Additionally, donor nerve availability is often insufficient for long nerve defects, further limiting reconstructive options (Kornfeld et al. 2019). A major challenge in these cases is the formation of scar tissue and adhesion around the repair site, which can result in nerve compression and suboptimal functional outcomes (Hussain et al. 2020). Various strategies, including both natural and synthetic nerve protectors, have been employed to shield injured nerves from the surrounding tissues (Thomson et al. 2022).

In this study, we aimed to assess the efficacy of different nerve protectors tested in a complex nerve injury model involving crush, transection, and end-to-end repair (CTR). Nerve protectors are designed to minimize scar formation, provide structural support, and reduce tension at the repair site. Studies have shown that nerve-wrapping techniques reduce the recurrence rates of nerve compression and

Department of Orthopaedics, University of Illinois at Chicago, Chicago, IL 60607, USA

✉ siemiom@uic.edu; siemiom@hotmail.com

scarring in reconstructive surgeries (Thakker et al. 2021). These protectors safeguard the nerve from external trauma while fostering optimal conditions for regeneration. Among natural protectors, the human amniotic membrane (hAM) is commonly used due to its neurotrophic properties, which promote nerve regeneration and functional recovery by modulating the expression of key neurotrophic factors (Botelho and Mamede 2015; Zhang et al. 2019). However, based on the literature reports, concerns were raised over the preservation and long-term stability of hAM (Leal-Marin et al. 2021).

In response to these challenges, we introduce the human epineurial patch (hEP) as a novel nerve protector, tested in an experimental rat model of complex sciatic nerve injury, to simulate challenging clinical scenarios after trauma. Derived from the epineurium of peripheral nerves, the hEP offers distinct advantages over traditional nerve protectors by reducing local inflammation, inhibiting fibrosis, and promoting axonal guidance as previously confirmed in our preliminary studies (Siemionow et al. 2011, 2017a, b, 2019, 2022; Kozłowska et al. 2022; Strojny et al. 2023). Unlike hAM, the hEP provides a more stable, biocompatible alternative specifically designed to optimally enhance nerve regeneration and improve functional recovery.

Therefore, we aimed to compare the effectiveness of hEP with that of hAM in enhancing nerve regeneration following the repair of complex nerve injuries. Furthermore, we expect that the application of hEP will result in improved nerve recovery compared with unprotected repair and the use of hAM as a wrapping material, thus establishing hEP as a promising alternative for optimizing nerve regeneration outcomes after traumatic injuries.

## 2. Materials and Methods

### 2.1. Experimental animals

The experimental procedures involving animals were conducted in strict accordance with protocols approved by the Institutional Animal Care and Use Committee (IACUC) of the University of Illinois at Chicago, which holds accreditation from the American Association for the Accreditation of Laboratory Animal Care (AAALAC). All animals were provided humane care in accordance with the *Principles of Laboratory Animal Care* established by the National Society for Medical Research, as well as the *Guide for the Care and Use of Laboratory Animal Resources*. A total of 36 athymic nude rats (CrI:NIH-Foxn1<sup>mu</sup>, Charles River Laboratories, Wilmington, MA, USA), each weighing between 150 g and 250 g, were selected for this study. The animals were housed in two per hooded cages at room temperature, maintained on a 14/10 light–dark schedule, and provided with water and irradiated rodent feed *ad libitum*.

### 2.2. Creation of the hEP

The human sciatic nerves used in this experimental study were provided by the Musculoskeletal Transplant Foundation (MTF; Edison, NJ, USA) to create hEP. Transported under sterile conditions on dry ice, the nerves were stored upon arrival in a (Glacier® Ultralow Temperature Freezer – Thermo Fisher Scientific, Waltham, MA, USA) set at  $-86^{\circ}\text{C}$ . The sciatic nerves were defrosted on a heating pad (T/Pump®, Gaymar Industries, Orchard Park, NY, USA) with warm water circulating at  $38^{\circ}\text{C}$ . Next, the hEP patches were created based on our well-established protocol, where 3–4 cm long sciatic nerve segments were further dissected, and the epineurium was separated from the fascicles under  $20\times$  magnification of the microsurgical microscope (Wild M-691, Leica Microsystems, Wetzlar, Germany) (Siemionow et al. 2011, 2017a, b, 2019, 2022; Kozłowska et al. 2022; Strojny et al. 2023). After dissection, each hEP was thoroughly inspected for any inadvertent damage, and the damaged samples were excluded from the study. Finally, the created hEP was divided into  $2\text{ cm} \times 1\text{ cm}$  patches and was submerged in saline until application into the sciatic nerve repair site following the CTR injury.

### 2.3. hAM

The hAM used in this study was obtained from the MTF, our longstanding collaborator. Both the AmnioBand® Viable and lyophilized AmnioBand Membrane (MTF Biologics, Edison, NJ, USA;  $2\text{ cm} \times 4\text{ cm}$ ; UPC: 840045712908) were processed following rigorous quality control protocols to ensure biological integrity. Transported under sterile, controlled conditions on dry ice to maintain low temperatures, the membranes were immediately stored upon arrival in a Glacier® Ultralow Temperature Freezer at  $-86^{\circ}\text{C}$  to preserve its viability and structural properties until further use.

### 2.4. Surgical procedure

Rats were anesthetized using 5% isoflurane (Terrell Isoflurane, Piramal Critical Care Inc., Bethlehem, PA, USA) in an induction chamber and maintained at 1.5%–2.5% using the Classic T3™ SurgiVet® Vaporizer (Smiths Medical ASD Inc., St. Paul, MI, USA). Buprenorphine SR (1.2 mg/kg) was administered subcutaneously 15 min prior to the incision for analgesia. Each rat was positioned on the left side, with the right hind limb shaved and hair removed using Nair™ (Church & Dwight Co., Inc., Ewing, NJ, USA). The surgical site was then cleansed with 5% povidone-iodine (Betadine®, Purdue Pharma L.P., Stamford, CO, USA), and the rats were placed on a warm water circulation heating pad (T/Pump®, Gaymar Industries). All procedures were performed aseptically under

20×–40× magnification of an operating microscope (Wild 691, Leica Microsystems). To expose the sciatic nerve, a 3 cm incision was made at the right gluteal region. Next, as previously described (Gudemez et al. 2002; Siemionow et al. 2011, 2017a, b, 2019, 2022; Kozłowska et al. 2022; Strojny et al. 2023), a standardized crush injury was applied to the sciatic nerve with a 5-inch straight mosquito hemostat (Walter Lorenz®, Jacksonville, FL, USA) for 5 min. The crushed segment of the sciatic nerve was resected with microsurgical scissors, followed by the standard end-to-end repair using 10-0 nylon sutures (Ethicon Inc., Raritan, NJ,

USA). Then, the nerve repair site was wrapped with either the hAM or hEP or was left without coverage as a control. Two additional 10-0 nylon sutures were used to secure the wrapping materials (Figure 1). The muscle layers were closed with 4-0 interrupted vicryl sutures, and the skin with 5-0 monocryl sutures (Ethicon). An antibiotic cream (Neosporin, Johnson & Johnson, USA – New Brunswick, NJ, USA) was applied to the incision site. Postoperative monitoring was conducted for 24 h to ensure normal recovery. Nerve samples were collected at both 6 weeks and 12 weeks after CTR for histological analysis.

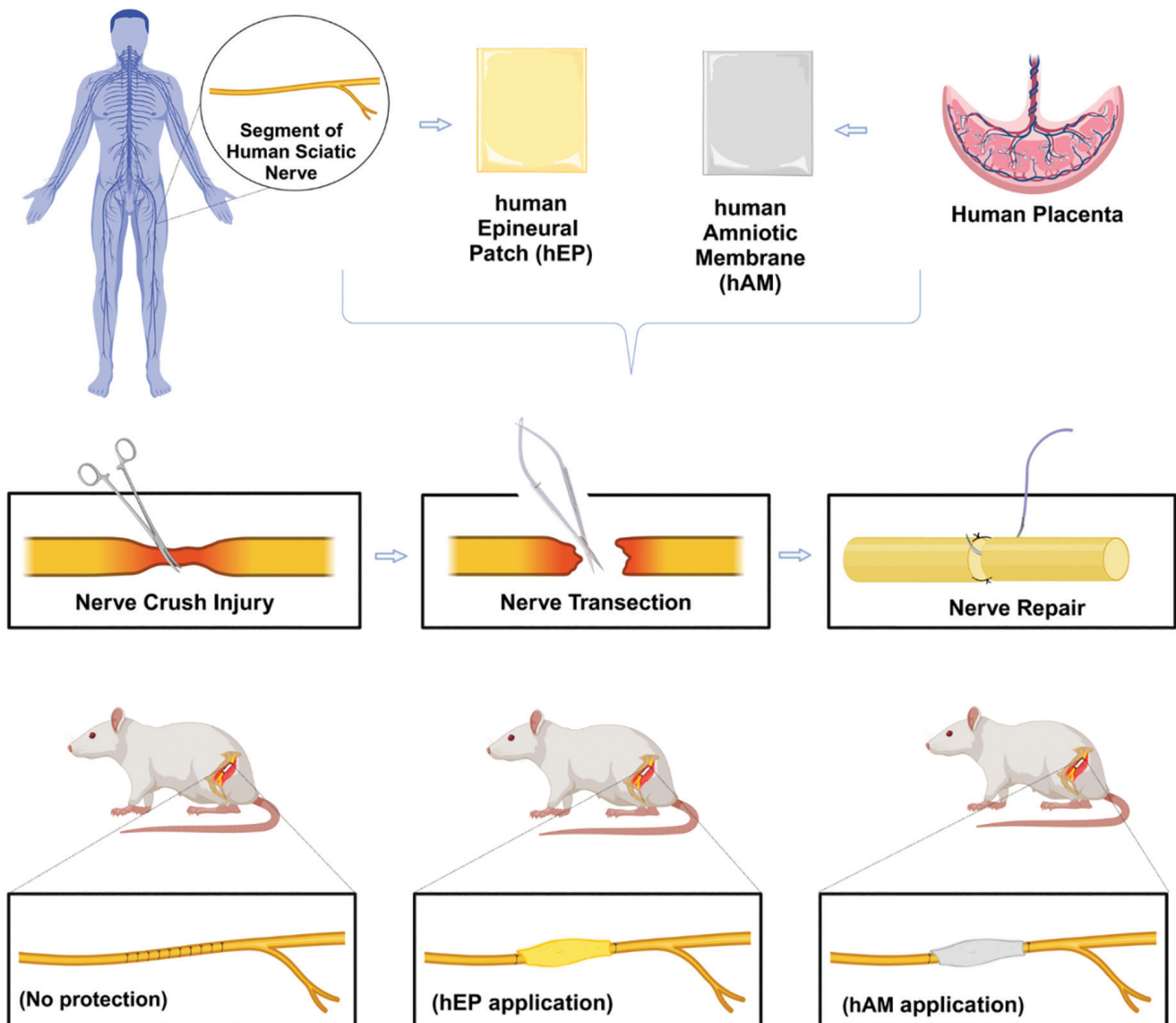


**Fig 1.** Schematic illustration of the experimental design detailing the creation and application of the hEP as an innovative approach to enhance nerve regeneration following sciatic nerve crush injury, transection, and end-to-end repair. hEP, human epineural patch; hAM, human amniotic membrane.

## 2.5. Postsurgical supportive treatment

Following the surgical procedure, each rat was kept in isolation with a protective collar to prevent self-inflicted wounds. After the initial 24-h period, the collar was removed, and the rats were returned to the original cages. Pain management was provided by administering buprenorphine (0.1 mg/kg) twice daily for the first 2 postoperative days. The surgical site was monitored daily for the first 14 days after surgery. Additionally, the overall wellbeing of the rats was assessed weekly by a board-certified veterinarian until study completion. Physical examinations of the animals assessed the signs of morbidity, changes in eating or drinking patterns, weight fluctuations, and mobility limitations. Additionally, rough hair or a hunched posture that could suggest that distress or pain was monitored closely.

## 2.6. Experimental groups

The study included 36 athymic nude rats (CrI:NIH-Foxn1<sup>nu</sup>), which were randomly assigned to six experimental groups of 6 rats each, divided into the 6-week and 12-week follow-up studies (Table 1). Each group underwent a CTR procedure, including sciatic nerve crush injury, followed by nerve transection and standard end-to-end repair. In the 6-week study, Group 1 served as the control and did not receive protection at the nerve repair site; Group 2: hEP patch was applied to the nerve repair site; and Group 3: hAM patch was applied to the nerve repair site. In the 12-week study, Groups 4–6 underwent the same CTR procedures as Groups 1–3, and were evaluated over the 12-week follow-up period (Figure 2).

## 2.7. Assessment methods

The animals were evaluated for functional recovery at specified time intervals: 1 week, 3 weeks, and 6 weeks in the 6-week study, and 1 week, 3 weeks, 6 weeks, 9 weeks, and 12 weeks in the 12-week study, following nerve CTR. Functional recovery assessments included the Toe-Spread test for motor recovery and the Pinprick test for sensory recovery. Samples were harvested at 6 weeks and 12 weeks post-surgery. The gastrocnemius muscle was harvested to assess muscle denervation atrophy using the standard gastrocnemius muscle index (GMI). Histomorphometric analysis of nerve samples harvested from the proximal, crushed, and distal sites quantified myelin thickness, axonal density, fiber diameter, and the percentage of myelinated nerve fibers.

**Table 1.** Experimental group descriptions and evaluation methods

Experimental group number	Repair method	Number of athymic nude rats per group
6 weeks study		
1	no protective wrapping	n=6
2	hEP	n=6
3	hAM	n=6
12 weeks study		
4	no protective wrapping	n=6
5	hEP	n=6
6	hAM	n=6
		Total number of athymic nude rats (n=36)

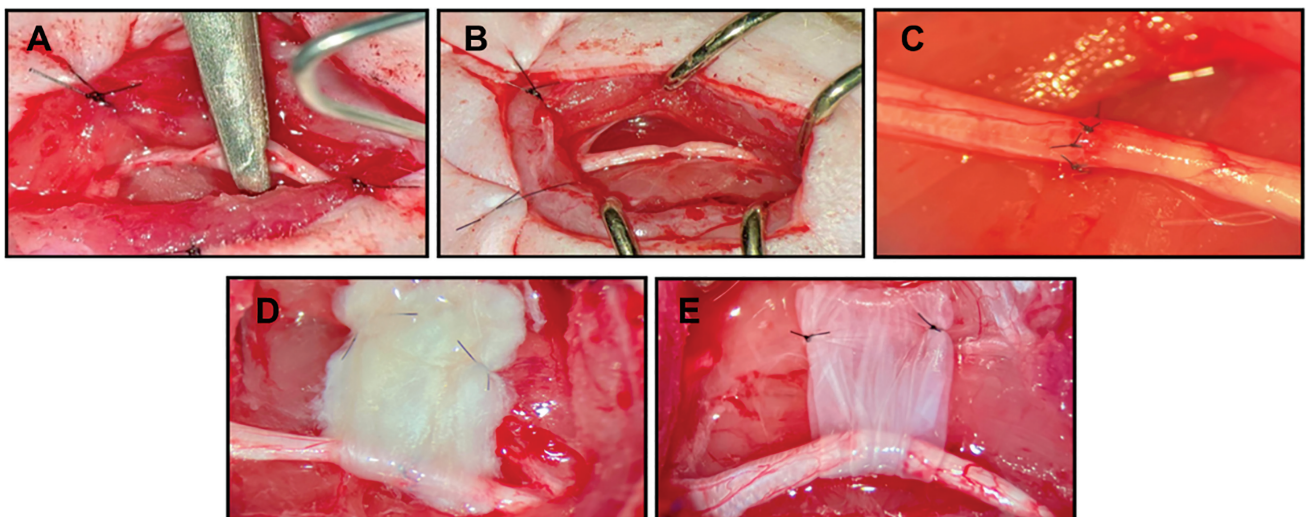


**Fig 2.** Surgical technique of the CTR procedure and application of the created hEP and hAM patch. (a) Creation of the sciatic nerve crush injury. (b) Sciatic nerve crush site 0.5 mm long. (c) End-to-end repair after resection of the sciatic nerve crush site. (d) Sciatic nerve repair site wrapped with the hEP. (e) Sciatic nerve repair site wrapped with the hAM. hAM, human amniotic membrane; hEP, human epineurial patch.



The neuroregenerative potential of hEP was further evaluated through immunostaining, analyzing the expression of selected neurogenic (Glial fibrillary acidic protein [GFAP], Laminin B, nerve growth factor [NGF], S-100), angiogenic (vascular endothelial growth factor [VEGF], von Willebrand factor [vWF]), and immunogenic (human leukocyte antigen-DR [HLA-DR], human leukocyte antigen class I [HLA-I]) markers.

## 2.8. Functional motor assessment with Toe-Spread test

The motor nerve recovery of the right sciatic nerve of each rat was evaluated using the Toe-Spread test. With an uninjured limb, the rat extends and abducts the hind foot toes when it is held up by the tail. To access this, the Toe-Spread test was graded on a scale of 0–3 points, based on the following guidelines: no movement was given 0 points; any sign of toe movement was assigned 1 point; abduction of the toes was graded with 2 points; and full toe extension and abduction, representing a normal response, was assigned a score of 3 points. This test was administered at least three times per evaluation point for every rat within each group at the designated time marks. The Toe-Spread test was done alongside the Pinprick test.

## 2.9. Functional sensory assessment with Pinprick test

Evaluation of the sensory nerve recovery was done using the Pinprick test. A pinching stimulus was applied to the skin of the rat's right hind limb, extending from the toe to the knee joint by using Adson's forceps (Walter Lorenz®) until limb withdrawal and/or a vocal response to the stimulus occurred. The stimulus was applied at a specific pressure and amount of time while targeting the skin without harming the deeper tissues. Sensory recovery was graded from 0 to 3 in the following manner: a score of 0 indicated no sensation in the limb, a score of 1 represented a withdrawal response between the knee and the ankle, a score of 2 represented a withdrawal response between the ankle and the toes, and a score of 3 represented a withdrawal response of the toes themselves. This test was performed at least three times per evaluation point for every rat within each group at the designated time marks. Following the Pinprick test, rats were closely monitored for signs of ecchymosis, wounds, edema, or changes in skin color, none of which were observed.

## 2.10. Macroscopic assessment of hEP and hAM at the sciatic nerve injury site

Macroscopic evaluation of the sciatic nerve injury site was conducted following euthanasia of the rats at the designated 6-week and 12-week endpoints using SomnaSol™

(Henry Schein Inc., Melville, NY, USA). Following euthanasia, right sciatic nerve segments – protected with either no wrapping, hEP, or hAM – were carefully harvested for histomorphometric and immunofluorescence analyses. A 3 cm incision was made in the gluteal region of the right hind limb to expose the sciatic nerve and the applied patches. The harvested samples were then evaluated for adhesion to the surrounding tissues; signs of local inflammation; and the structural integrity, shape, and appearance of the patches. Additionally, assessments were made for the presence of fascicle-like structures within the hEP or hAM, signs of nerve atrophy distal to the hEP or hAM, and vascularization of the patches to determine the extent of healing and regeneration at the injury site.

## 2.11. Assessment of muscle denervation atrophy

The gastrocnemius muscles were harvested for macroscopic assessment, and muscle denervation atrophy was evaluated using the GMI at the 6-week and 12-week follow-ups. The wet weight of the gastrocnemius muscle was measured using an analytical balance Ohaus Precision Standard (Ohaus Corporation, USA – Parsippany, NJ, USA). The GMI was calculated as the ratio of the wet weight of the gastrocnemius muscle on the operated side to that of the contralateral gastrocnemius muscle on the unoperated side. Recovery from denervation atrophy was expressed as a percentage value, with a GMI of 100% indicating full recovery of the gastrocnemius muscle on the operated side.

## 2.12. Histomorphometric analysis

The sciatic nerve samples from the proximal, crushed, and distal nerve segments with either No protection, hEP, or hAM application were excised, immersed in, and fixed with 2.5% glutaraldehyde. Post-fixation was performed using 4% aqueous osmium tetroxide according to the manufacturer's protocol. For histological analysis, 1  $\mu\text{m}$  thick cross-sections were stained with Toluidine Blue Solution (Thermo Fisher Scientific, Waltham, MA, USA). These sections were examined under a light microscope (Leica DM 5500B Automated Upright Microscope, RRID: SCR\_020219, Leica Microsystems) using a high-magnification objective lens (100 $\times$ ) and captured with a digital camera (Leica DFC290 HD Color Digital FireWire Camera, Leica Microsystems). Images were analyzed using Image-Pro Plus (Media Cybernetics, Rockville, MD, USA). Six nonoverlapping fields were selected from each nerve section for quantification. Parameters such as myelin thickness ( $\mu\text{m}$ ), axonal density (axons/ $\mu\text{m}^2$ ), fiber diameter ( $\mu\text{m}$ ), and the percentage of myelinated nerve fibers (%) were measured using ImageJ software (Wayne Rasband, National Institutes of Health, Bethesda, MD, USA; RRID: SCR\_003070), focusing exclusively on myelinated nerve fibers.

### 2.13. Immunostaining assessment

Immunofluorescent staining was used to assess the expression of selected neurogenic (S-100, NGF, GFAP, Laminin B), angiogenic (vWF, VEGF), and immunogenic (MHC class I and II) markers within nerve samples. The paraffin sections of the crush and distal nerve segments were mounted onto glass slides and underwent deparaffinization with xylene, followed by subsequent rinsing in ethanol and distilled water. The slides were then rinsed with Tris Buffered Saline (TBS) Tween 0.1% (TBS, Agilent Technologies, Inc., USA – Santa Clara, CA, USA) for 2 min on an orbital shaker, fixed with cold acetone for 8 min, and watched three times with TBS-Tween 0.1% for 5 min each on an orbital shaker. Following blocking with Goat serum at 10% for 1 h at 4°C, the nerve samples were incubated at 4°C overnight in dark with antibody diluent (1:50) and the following primary antibodies: S-100 (S100 4C4.9, RRID: AB\_795376, Invitrogen, Waltham, MA, USA), NGF (Anti-NGF beta, RRID: AB\_10856084, Bioss Antibodies, Woburn, MA, USA), GFAP (anti-GFAP, ab68428, RRID: AB\_1209224, Abcam, Cambridge, UK), Laminin B (Laminin, RRID: AB\_2133633, Invitrogen, USA – Waltham, MA, USA), vWF (vWF, RRID: AB\_10642840, Proteintech, Rosemont, IL, USA), VEGF (anti-VEGF VG1, RRID: AB\_10001947, Novus Biologicals, Englewood, CO, USA), MHC class I (HLA class I APC, RRID: AB\_1557426, Proteintech, USA – Rosemont, IL, USA), and MHC class II (BD Pharmingen™ Purified HLA-DR, DP, DQ, RRID: AB\_395939, BD Biosciences, Franklin Lakes, NJ, USA). The primary antibodies were selected and combined to perform co-staining. Next, the samples were rinsed three times with TBS for 5 min each on an Orbital shaker. The secondary antibodies (IgG Alexa Fluor™ 488, RRID: AB\_2534069, Invitrogen, USA – Waltham, MA, USA) (IgG Alexa Fluor® 594, ab150132, RRID: AB\_2810222, Abcam, UK – Cambridge, UK) were diluted in antibody diluent (1:500). The secondary antibodies application was performed in dark condition and followed by a 1-h incubation at 4°C in a humidity chamber. The slides were rinsed in TBS three times for 5 min each and mounted with Fluoromount-G® (Southern Biotech, Birmingham, AL, USA). The slides were assessed using an upright confocal microscope (Leica TCS SP2 Upright Confocal Microscope, RRID SCR\_020231, Leica Microsystems) with a digital camera (QImaging® Retiga-2000R Charge Coupled Device, QImaging, British Columbia, Canada) and ImagePro Plus (RRID SCR\_016879) – Media Cybernetics, USA – Rockville, MD, USA software. Evaluation of immunofluorescence was scored based on signal intensity as follows: 0 = no staining, 1 = weak, 2 = moderate, and 3 = strong.

### 2.14. Statistical analysis

Statistical analyses were performed using GraphPad Prism software (RRID: SCR\_002798, GraphPad Software,

San Diego, CA, USA). One- or two-way ANOVA tests were conducted to assess statistical significance, followed by Tukey's *post hoc* test for multiple group comparisons. Data from *in vitro* experiments, which included six randomly selected nerve samples, are presented as mean  $\pm$  standard error of the mean (SEM). Statistical significance was defined as  $p < 0.05$ , with significance levels indicated by asterisks: \* $p < 0.05$ , \*\* $p < 0.01$ , \*\*\* $p < 0.001$ , and \*\*\*\* $p < 0.0001$ .

## 3. Results

### 3.1. Confirmation of sciatic nerve motor function improvement following hEP application

**At the 6-week follow-up**, no significant motor response was observed at the 1-week time point across all groups, with the No protection, hEP, and hAM groups showing minimal or no measurable response ( $0.000 \pm 0.000$ ,  $p > 0.05$ ). By 3 weeks, the hEP improved motor function compared with the No protection and hAM groups ( $0.778 \pm 0.319$ ,  $p < 0.05$  vs.  $0.222 \pm 0.319$  and  $0.000 \pm 0.000$ , respectively). At 6 weeks, the hEP group exhibited the highest motor response, significantly outperforming the No protection and hAM groups ( $2.165 \pm 0.320$ ,  $p < 0.05$  vs.  $1.167 \pm 0.320$  and  $1.390 \pm 0.320$ , respectively; Figure 3a).

**At the 12-week follow-up**, all groups showed minimal or no measurable response at the 1-week and 3-week time points, with no significant differences between No protection, hEP, and hAM ( $0.000 \pm 0.000$  for all groups,  $p > 0.05$ ). By 6 weeks, hEP exhibited a significantly higher motor response compared with No Protection ( $1.777 \pm 0.262$  vs.  $0.833 \pm 0.262$ ,  $p < 0.01$ ), though the difference between hEP and hAM did not reach statistical significance ( $1.777 \pm 0.262$  vs.  $1.167 \pm 0.262$ ,  $p > 0.05$ ). At 9 weeks, hEP continued to show superior motor recovery compared with No Protection ( $2.278 \pm 0.262$  vs.  $1.112 \pm 0.262$ ,  $p < 0.0001$ ), while the difference between hEP and hAM remained nonsignificant ( $2.278 \pm 0.262$  vs.  $1.722 \pm 0.262$ ,  $p > 0.05$ ). By 12 weeks, hEP demonstrated the highest level of motor function recovery ( $2.500 \pm 0.262$ ), significantly outperforming No Protection ( $1.667 \pm 0.262$ ,  $p < 0.01$ ), while no significant difference was observed between hEP and hAM ( $2.057 \pm 0.262$ ,  $p > 0.05$ ) (Figure 4a).

### 3.2. Confirmation of enhanced sciatic nerve sensory recovery following hEP application

**At the 6-week follow-up**, no differences were observed between the No protection, hEP, and hAM groups. By 3 weeks, the hEP group showed a significantly better recovery compared with the hAM group ( $1.667 \pm 0.201$  vs.  $1.112 \pm 0.201$ ,  $p < 0.05$ ), but no significant difference was found between

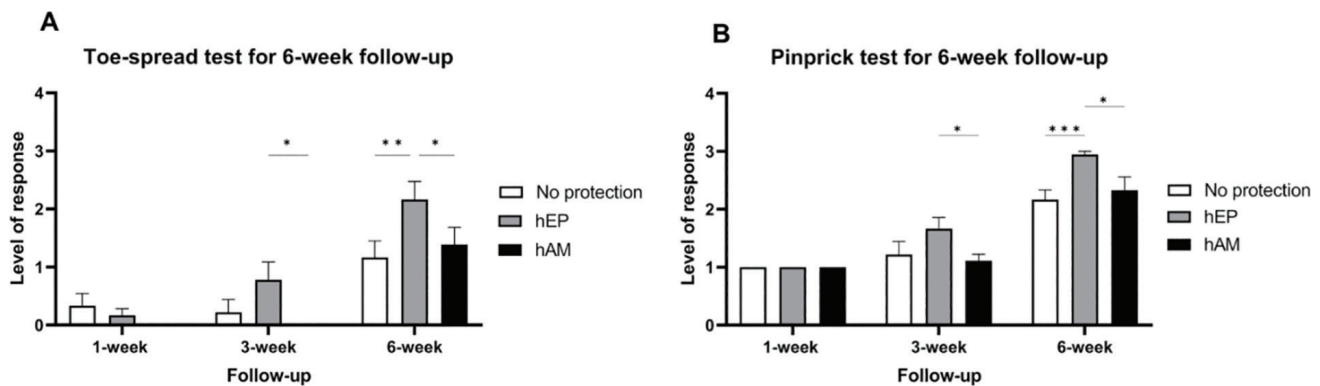


**Fig 3.** Functional assessment of sciatic nerve regeneration was done using Toe-Spread and Pinprick tests in the 6-week study at 1, 3, and 6-week study points. (a) Motor recovery (Toe-Spread test) revealed no significant response at 1 week, but the hEP group showed significant improvement by 3 weeks and the highest motor response at 6 weeks. (b) Sensory recovery (Pinprick test) showed significantly better outcomes in the hEP group at 3 weeks and 6 weeks compared with the No protection and hAM groups, with the hEP group demonstrating the highest response at 6 weeks. Data are presented as mean ± SEM, with significance indicated as \* $p < 0.05$ , \*\* $p < 0.01$ , \*\*\* $p < 0.001$ , \*\*\*\* $p < 0.0001$ . hAM, human amniotic membrane; hEP, human epineural patch; SEM, standard error of the mean.

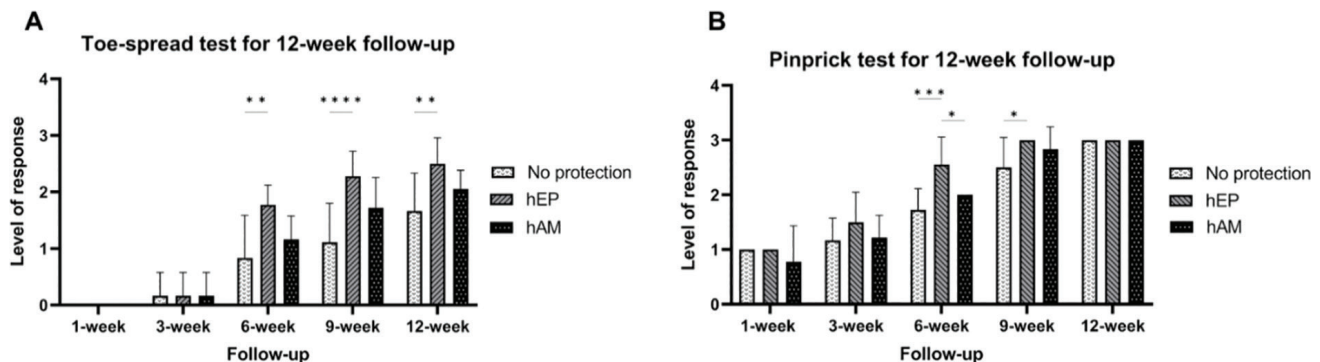


**Fig 4.** Functional assessment of sciatic nerve regeneration was done using Toe-Spread and Pinprick tests in the 12-week study at 1, 3, 6, and 12-week study points. (a) Motor recovery (Toe-Spread test) showed minimal response across all groups at 3 weeks. By 6 weeks, the hEP group maintained significantly higher response levels than the No protection group. By 9 weeks, the hEP group outperformed both groups, though statistical differences were observed for No protection. At 12 weeks, the hEP group achieved the highest recovery, significantly outperforming the No protection group. (b) Sensory recovery (Pinprick test) revealed that the hEP group had significantly higher responses at 6 weeks and 9 weeks than the other groups, with comparable recovery observed across all groups by 12 weeks. Data are mean ± SEM, with significance marked as \* $p < 0.05$ , \*\* $p < 0.01$ , \*\*\* $p < 0.001$ , and \*\*\*\* $p < 0.0001$ . hAM, human amniotic membrane; hEP, human epineural patch; SEM, standard error of the mean.

hEP and No protection ( $p > 0.05$ ). At 6 weeks, the hEP group demonstrated the highest recovery, significantly outperforming both the No protection ( $2.945 \pm 0.201$  vs.  $2.167 \pm 0.201$ ,  $p < 0.01$ ) and hAM groups ( $2.945 \pm 0.201$  vs.  $2.332 \pm 0.201$ ,  $p < 0.05$ ; Figure 3b).

**At the 12-week follow-up**, the hEP group continued to show superior recovery outcomes. At 6 weeks, the hEP group demonstrated significantly better recovery compared with No protection ( $2.555 \pm 0.207$  vs.  $1.723 \pm 0.207$ ,  $p < 0.001$ ) and hAM ( $2.555 \pm 0.207$  vs.  $2.000 \pm 0.207$ ,  $p < 0.05$ ). By 9 weeks, the hEP group continued to show superior recovery, significantly outperforming No protection ( $3.000 \pm 0.207$  vs.  $2.500 \pm 0.207$ ,  $p < 0.05$ ). At the 12-week mark, recovery outcomes were comparable across all groups, with no statistically significant differences ( $3.000 \pm 0.207$  for all,  $p > 0.05$ ) (Figure 4b).

### 3.3. Confirmation of reduced inflammation, adhesion, and fibrosis following hAM and hEP application

During nerve sample harvesting at 6-week and 12-week study end-points, the evaluation of the repair site after the CTR procedure revealed no signs of adhesion, fibrosis, or local inflammatory response around the hEP application. Remarkably, fascicle-like structures were visible at the site of the CTR procedure. Specifically, at the application site, the hEP demonstrated preserved structural integrity and morphology, displaying adequate vascularization. In contrast, the hAM was difficult to detect at the site of application during the CTR procedure upon macroscopic evaluation at both the 6-week and 12-week following nerve repair.

### 3.4. Confirmation of improved muscle morphology and reduced denervation atrophy following hEP application

**At the 6-week follow-up**, the hEP group had higher GMI values compared with the hAM and No protection groups, though these differences were not statistically significant (Figure 5a).

**At the 12-week follow-up**, the hEP group showed a significant improvement with a GMI value of  $0.955 \pm 0.014$ , which was notably higher than the no protective wrapping group's GMI of  $0.857 \pm 0.030$  ( $p < 0.05$ ). Additionally, the hEP group had higher GMI values compared with the hAM group, which had a GMI of  $0.903 \pm 0.015$ ; however, this difference was not statistically significant ( $p > 0.05$ ) (Figure 5b).

### 3.5. Confirmation of sciatic nerve fiber regeneration following hEP application

The efficacy of hEP was evaluated by assessing myelin thickness, fiber diameter, percentage of myelinated fibers, and axonal density at 6 weeks (Figure 6) and 12 weeks (Figure 7) following nerve CTR injury.

#### 3.5.1. Confirmation of increased myelin thickness following hEP application

**At the 6-week follow-up**, the analysis of myelin thickness revealed significant findings. At the proximal site, significant differences were observed between the No protection group and the hEP group ( $2.315 \pm 0.024 \mu\text{m}$  vs.  $3.267 \pm 0.043 \mu\text{m}$ ,  $p < 0.0001$ ), as well as between the No protection and hAM

groups ( $2.315 \pm 0.024 \mu\text{m}$  vs.  $2.672 \pm 0.020 \mu\text{m}$ ,  $p < 0.0001$ ), and between the hEP and hAM groups ( $3.267 \pm 0.043 \mu\text{m}$  vs.  $2.672 \pm 0.020 \mu\text{m}$ ,  $p < 0.0001$ ; Figure 6a). At the crushed nerve site, the group without protective wrapping had a significantly lower myelin thickness compared with the hEP group ( $0.829 \pm 0.088 \mu\text{m}$  vs.  $1.153 \pm 0.010 \mu\text{m}$ ,  $p < 0.0001$ ) and the hAM group ( $0.829 \pm 0.088 \mu\text{m}$  vs.  $1.381 \pm 0.013 \mu\text{m}$ ,  $p < 0.0001$ ). A significant difference was also noted between the hEP and hAM groups ( $1.153 \pm 0.010 \mu\text{m}$  vs.  $1.381 \pm 0.013 \mu\text{m}$ ,  $p < 0.0002$ ; Figure 6b). At the distal site, the No protection group again had significantly lower myelin thickness compared with the hEP group ( $0.931 \pm 0.011 \mu\text{m}$  vs.  $1.250 \pm 0.011 \mu\text{m}$ ,  $p < 0.0001$ ) and the hAM group ( $0.931 \pm 0.011 \mu\text{m}$  vs.  $1.775 \pm 0.063 \mu\text{m}$ ,  $p < 0.0001$ ), with a significant difference between the hEP and hAM groups ( $1.250 \pm 0.011 \mu\text{m}$  vs.  $1.775 \pm 0.063 \mu\text{m}$ ,  $p < 0.0001$ ; Figure 6c).

**At the 12-week follow-up**, statistically significant differences were again observed across the groups. At the proximal site, the hEP group exhibited significantly greater myelin thickness compared with the No protection group ( $2.516 \pm 0.024 \mu\text{m}$  vs.  $3.480 \pm 0.019 \mu\text{m}$ ,  $p < 0.0001$ ) and the hAM group ( $2.516 \pm 0.024 \mu\text{m}$  vs.  $2.361 \pm 0.025 \mu\text{m}$ ,  $p < 0.0001$ ), with significant differences also noted between the hEP and hAM groups ( $3.480 \pm 0.019 \mu\text{m}$  vs.  $2.361 \pm 0.025 \mu\text{m}$ ,  $p < 0.0001$ ; Figure 7a). At the crushed site, the hEP group had significantly greater myelin thickness compared with the No protection group ( $1.038 \pm 0.008 \mu\text{m}$  vs.  $1.572 \pm 0.012 \mu\text{m}$ ,  $p < 0.0001$ ) and the hAM group ( $1.038 \pm 0.008 \mu\text{m}$  vs.  $1.646 \pm 0.010 \mu\text{m}$ ,  $p < 0.0001$ ), with significant differences also noted between the hEP and hAM groups ( $1.572 \pm 0.012 \mu\text{m}$  vs.  $1.646 \pm 0.010 \mu\text{m}$ ,  $p < 0.0001$ ; Figure 7b). At the distal site, the hEP group showed significantly higher myelin

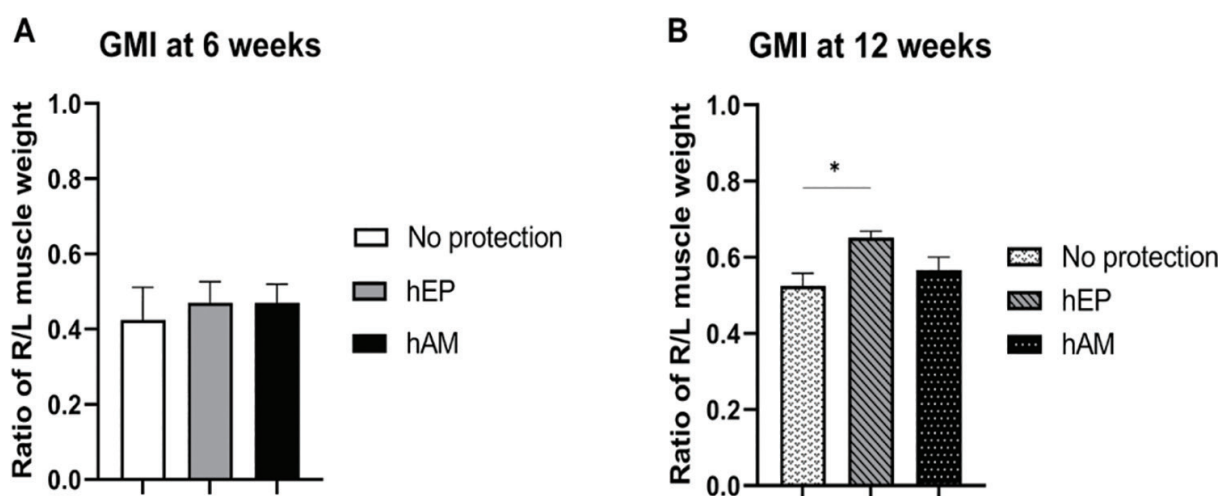


**Fig 5.** Evaluation of muscle denervation atrophy by GMI. (a) At 6 weeks, no significant differences in the GMI were observed between groups. (b) In contrast, at 12 weeks, the hEP group exhibited a significantly higher GMI compared with the No protection group. Data are presented as mean  $\pm$  SEM. Statistical significance was determined using a one-way ANOVA test for group comparisons, with significance levels as follows: \* $p < 0.05$ , \*\* $p < 0.01$ , \*\*\* $p < 0.001$ , and \*\*\*\* $p < 0.0001$ . GMI, gastrocnemius muscle index; hAM, human amniotic membrane; hEP, human epineural patch; SEM, standard error of the mean.



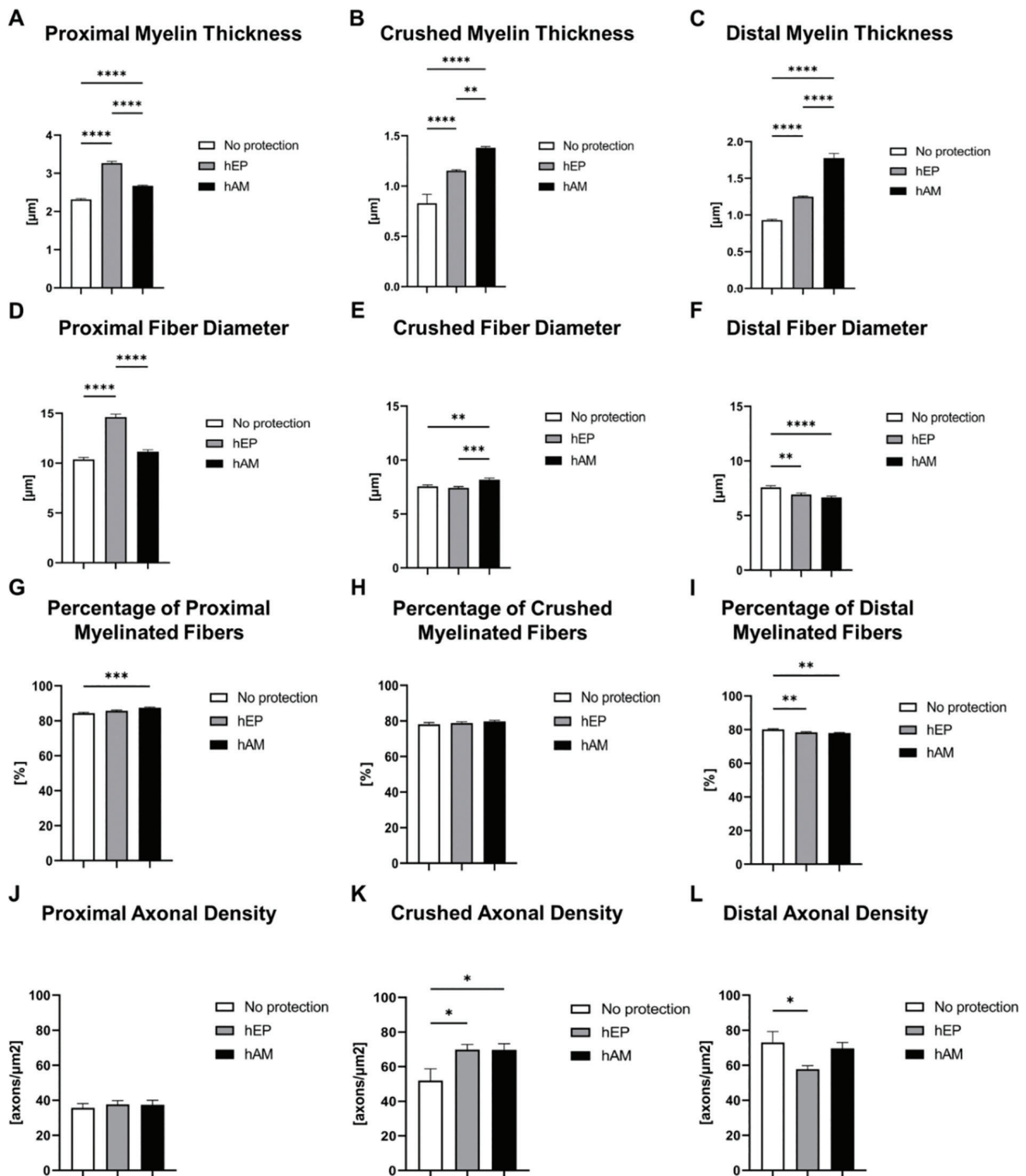


**Fig 6.** Histological assessment of the proximal, crushed, and distal parts of the injured segment at 6 weeks after sciatic nerve crush injury followed by nerve transection and end-to-end repair. (a) Proximal myelin thickness, (b) Crushed myelin thickness, (c) Distal myelin thickness, (d) Proximal fiber diameter, (e) Crushed fiber diameter, (f) Distal fiber diameter, (g) Percentage of proximal myelinated fibers, (h) Percentage of crushed myelinated fibers, (i) Percentage of distal myelinated fibers, (j) Proximal axonal density, (k) Crushed axonal density, and (l) Distal axonal density. The data are presented as mean  $\pm$  SEM and statistical significance was determined using a one-way ANOVA test for group comparisons, with significance levels denoted as \* $p < 0.05$ , \*\* $p < 0.01$ , \*\*\* $p < 0.001$ , and \*\*\*\* $p < 0.0001$ . hAM, human amniotic membrane; hEP, human epineural patch; SEM, standard error of the mean.

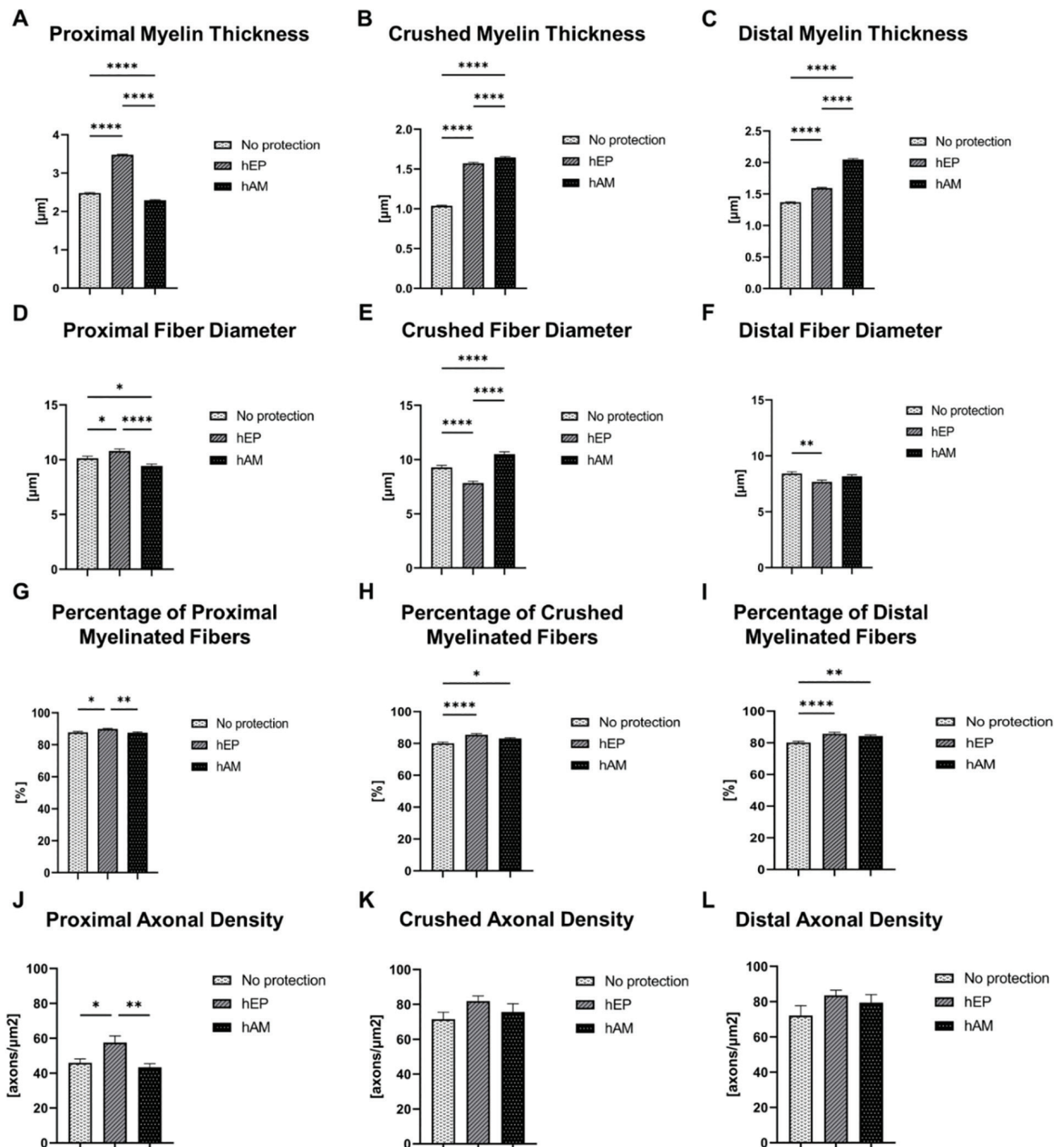


**Fig 7.** Histological assessment of the proximal, crushed, and distal parts of the injured segment at 12 weeks after sciatic nerve crush injury followed by nerve transection and end-to-end repair. (a) Proximal myelin thickness, (b) Crushed myelin thickness, (c) Distal myelin thickness, (d) Proximal fiber diameter, (e) Crushed fiber diameter, (f) Distal fiber diameter, (g) Percentage of proximal myelinated fibers, (h) Percentage of crushed myelinated fibers, (i) Percentage of distal myelinated fibers, (j) Proximal axonal density, (k) Crushed axonal density, and (l) Distal axonal density. The data are presented as mean  $\pm$  SEM and statistical significance was determined using a one-way ANOVA test for group comparisons, with significance levels denoted as \* $p < 0.05$ , \*\* $p < 0.01$ , \*\*\* $p < 0.001$ , and \*\*\*\* $p < 0.0001$ . hAM, human amniotic membrane; hEP, human epineural patch; SEM, standard error of the mean.

thickness than the No protection group ( $1.355 \pm 0.009 \mu\text{m}$  vs.  $1.597 \pm 0.010 \mu\text{m}$ ,  $p < 0.0001$ ) and the hAM group ( $1.355 \pm 0.009 \mu\text{m}$  vs.  $2.048 \pm 0.012 \mu\text{m}$ ,  $p < 0.0001$ ), with significant differences also observed between the hEP and hAM groups ( $1.597 \pm 0.010 \mu\text{m}$  vs.  $2.048 \pm 0.012 \mu\text{m}$ ,  $p < 0.0001$ ; Figure 7c).

### 3.5.2. Confirmation of increased sciatic nerve fiber diameters following hEP application

**At the 6-week follow-up**, in the proximal site, the hEP group exhibited a significantly larger fiber diameter compared with both the No protection and hAM groups. The No protection group ( $14.613 \pm 0.309 \mu\text{m}$ ) showed a highly significant difference compared with the hEP group ( $10.363 \pm 0.201 \mu\text{m}$ ,  $p < 0.0001$ ). Additionally, the hEP group displayed a significant difference in fiber diameter when compared with the hAM group ( $11.144 \pm 0.203 \mu\text{m}$ ,  $p < 0.0001$ ) (Figure 6d). In the crushed section, the hAM group achieved the most promising results, with a fiber diameter of ( $8.179 \pm 0.153 \mu\text{m}$ ), significantly outperforming both the No protection group ( $7.557 \pm 0.131 \mu\text{m}$ ) and the hEP group ( $7.422 \pm 0.125 \mu\text{m}$ ,  $p < 0.0001$ ; Figure 6e). In the distal section, the No protection group exhibited the most favorable outcomes, with a fiber diameter of ( $7.576 \pm 0.149 \mu\text{m}$ ), significantly surpassing both the hEP group ( $6.934 \pm 0.125 \mu\text{m}$ ) and the hAM group ( $6.656 \pm 0.125 \mu\text{m}$ ; Figure 6f).

**At the 12-week follow-up**, the assessment revealed significant differences across all treatment groups, varying by nerve region. In the proximal region, the hEP group showed the largest mean fiber diameter ( $10.788 \pm 0.197 \mu\text{m}$ ), followed by the No protection group ( $10.127 \pm 0.197 \mu\text{m}$ ) and the hAM group ( $9.434 \pm 0.177 \mu\text{m}$ ). Statistical analysis confirmed significant differences between the hEP and No protection groups ( $p < 0.05$ ) and between the hEP and hAM groups ( $p < 0.0001$ ; Figure 7d). In the crushed region, the hAM group demonstrated the largest mean fiber diameter ( $10.508 \pm 0.207 \mu\text{m}$ ), followed by the No protection group ( $9.282 \pm 0.185 \mu\text{m}$ ) and the hEP group ( $7.838 \pm 0.167 \mu\text{m}$ ). Significant differences were observed among all groups, with the hAM group showing significantly larger fiber diameters compared with both the No protection and hEP groups ( $p < 0.0001$ ; Figure 7e). In the distal region, the No protection group exhibited the largest mean fiber diameter ( $8.417 \pm 0.171 \mu\text{m}$ ), followed by the hAM group ( $8.160 \pm 0.154 \mu\text{m}$ ) and the hEP group ( $7.670 \pm 0.165 \mu\text{m}$ ). Statistical analysis revealed a significant difference between the No protection and hEP groups ( $p < 0.01$ ; Figure 7f).

### 3.5.3. Confirmation of increased percentage of myelinated fibers following hEP and hAM application

**At the 6-week follow-up**, in the proximal region, the hAM group exhibited the highest percentage of myelinated

fibers ( $87.425\% \pm 0.474\%$ ), followed by the hEP group ( $85.706\% \pm 0.515\%$ ), with the No protection group displaying the lowest percentage ( $84.339\% \pm 0.536\%$ ). Statistical analysis revealed a significant difference between the hAM and No protection groups ( $p < 0.001$ ), although the comparison between the hEP group and the other two groups did not reach statistical significance (Figure 6g). Similarly, in the crushed region, no significant differences were observed among the groups, as the percentage of myelinated fibers was comparable:  $79.809\% \pm 0.585\%$  in the hAM group,  $78.863\% \pm 0.644\%$  in the hEP group, and  $78.092\% \pm 1.003\%$  in the No protection group. ANOVA analysis confirmed no statistical significance ( $p > 0.05$ ; Figure 6h). Conversely, in the distal region, the No protection group had a significantly higher percentage of myelinated fibers ( $80.160\% \pm 0.383\%$ ) compared with both the hEP ( $78.350\% \pm 0.474\%$ ,  $p < 0.01$ ) and hAM groups ( $77.989\% \pm 0.334\%$ ,  $p < 0.001$ ; Figure 6i).

**At the 12-week follow-up**, significant differences were observed across nerve regions when comparing hEP and hAM treatments with No protection. In the proximal region, the hEP group exhibited the highest myelinated fiber percentage ( $89.841\% \pm 0.453\%$ ), significantly surpassing both the No protection ( $87.775\% \pm 0.590\%$ ) and hAM ( $87.559\% \pm 0.477\%$ ) groups ( $p < 0.01$ ). The difference between the hEP and No protection groups was also statistically significant ( $p < 0.05$ ; Figure 7g). Additionally, in the crushed region, the hEP group demonstrated the highest myelinated fiber percentage ( $85.408\% \pm 0.825\%$ ), significantly outperforming the No protection ( $80.123\% \pm 0.710\%$ ) and hAM ( $83.111\% \pm 0.509\%$ ) groups ( $p < 0.0001$ ). Significant differences were noted between the No protection and hEP groups ( $p < 0.0001$ ) and between the No protection and hAM groups ( $p < 0.05$ ; Figure 6h). Furthermore, in the distal region, both the hEP ( $85.712\% \pm 0.956\%$ ) and hAM groups ( $84.315\% \pm 0.646\%$ ) showed significantly higher percentages of myelinated fibers compared with the No protection group ( $80.157\% \pm 0.772\%$ ,  $p < 0.0001$ ). Significant differences were observed between the No protection and hEP groups ( $p < 0.0001$ ) and between the No protection and hAM groups ( $p < 0.01$ ; Figure 7i).

### 3.5.4. Confirmation of increased axonal density at the crush repair site following hEP application

**At the 6-week follow-up**, in the proximal nerve segment, no statistically significant differences in axonal density were observed among the groups, with similar values recorded for the No protection ( $35.688 \pm 2.446 \text{ axons}/\mu\text{m}^2$ ), hEP ( $37.706 \pm 2.130 \text{ axons}/\mu\text{m}^2$ ), and hAM ( $37.389 \pm 2.033 \text{ axons}/\mu\text{m}^2$ ) groups (Figure 6j). In contrast, at the crushed site, the hEP group demonstrated a significantly higher axonal density ( $69.889 \pm 3.005 \text{ axons}/\mu\text{m}^2$ ) compared with the No protection group ( $51.944 \pm 6.863 \text{ axons}/\mu\text{m}^2$ ,  $p < 0.05$ ). Similarly, the hAM group showed a marked increase in axonal density

( $69.722 \pm 3.542$  axons/ $\mu\text{m}^2$ ) relative to the No protection group, with statistical significance ( $p < 0.05$ ; Figure 6k). At the distal site, the No protection group exhibited the highest axonal density ( $73.000 \pm 6.255$  axons/ $\mu\text{m}^2$ ), significantly surpassing the hEP group ( $57.778 \pm 2.041$  axons/ $\mu\text{m}^2$ ,  $p < 0.05$ ), while no significant difference was found between the No protection and hAM groups ( $69.611 \pm 3.469$  axons/ $\mu\text{m}^2$ ) at this location (Figure 6l).

**At the 12-week follow-up**, in the proximal segment, the hEP group exhibited significantly higher axonal density ( $57.556 \pm 3.844$  axons/ $\mu\text{m}^2$ ) compared with both the No protection ( $45.944 \pm 2.289$  axons/ $\mu\text{m}^2$ ) and hAM ( $43.389 \pm 2.076$  axons/ $\mu\text{m}^2$ ) groups, with strong statistical significance ( $p < 0.001$ ) (Figure 7j). In the crushed region, the hEP group also showed an increase in axonal density ( $81.833 \pm 3.026$  axons/ $\mu\text{m}^2$ ) compared with the No protection group ( $71.500 \pm 4.026$  axons/ $\mu\text{m}^2$ ), although this difference was not statistically significant. Similarly, while the hAM group ( $75.722 \pm 4.617$  axons/ $\mu\text{m}^2$ ) outperformed the No protection group, the difference did not reach statistical significance ( $p > 0.05$ ) (Figure 7k). At the distal site, the hEP group ( $83.500 \pm 3.065$  axons/ $\mu\text{m}^2$ ) exhibited a higher axonal density than the hAM group ( $79.444 \pm 4.620$  axons/ $\mu\text{m}^2$ ) but was lower than the No protection group ( $72.111 \pm 5.5860$  axons/ $\mu\text{m}^2$ ). Statistical analysis revealed no significant differences between the groups in this region ( $p > 0.05$ ) (Figure 7l).

### 3.6. Confirmation of neuroregenerative potential of hEP

To evaluate the neuroregenerative potential of the hEP, selected neurogenic (GFAP, Laminin B, NGF, S-100), angiogenic (VEGF, vWF) and immunogenic (HLA-DR, HLA-I) markers were assessed following the nerve CTR injury model (Figures 8 and 9).

#### 3.6.1. Confirmation of increased GFAP expression at crush repair site following hEP application

**At the 6-week follow-up**, GFAP expression at the crush site was significantly higher in the hAM group ( $2.833 \pm 0.167$ ) compared with the hEP ( $2.583 \pm 0.083$ ) and No protection groups ( $1.083 \pm 0.363$ ;  $p < 0.001$ ). The hEP group also showed significantly higher expression compared with the No protection group ( $2.583 \pm 0.083$  vs.  $1.083 \pm 0.363$ ;  $p < 0.001$ ). In the distal region, GFAP expression was comparable between the No protection and hEP groups ( $1.583 \pm 0.220$  for both), while the hAM group exhibited higher expression ( $2.333 \pm 0.167$ ), though this difference was not statistically significant (Figure 8a).

**At the 12-week follow-up**, GFAP expression at the crush site was highest in the No protection group ( $1.667 \pm 0.167$ ), followed by the hEP ( $1.500 \pm 0.500$ ) and hAM groups ( $0.667 \pm 0.333$ ;  $p > 0.05$ ). In the distal region, the hEP group

showed the highest expression ( $1.333 \pm 0.167$ ) compared with the hAM ( $0.750 \pm 0.382$ ) and No protection groups ( $0.667 \pm 0.167$ ;  $p > 0.05$ ) (Figure 9a).

#### 3.6.2. Confirmation of increased Laminin B Expression at the crush repair site following hEP application

**At the 6-week follow-up**, Laminin B expression in the crush region was increased in the hEP group ( $1.250 \pm 0.144$ ) compared with the hAM ( $1.167 \pm 0.441$ ) and No protection groups ( $0.500 \pm 0.500$ ), but these differences were not statistically significant ( $p > 0.05$ ). Similarly, in the distal region, the hEP group showed slightly higher expression ( $1.000 \pm 0.289$ ) than the hAM ( $0.917 \pm 0.220$ ) and No protection groups ( $0.833 \pm 0.167$ ), with no significant differences observed between groups ( $p > 0.05$ ) (Figure 8b).

**At the 12-week follow-up**, Laminin B expression at the crush site was significantly higher in the hEP group ( $2.083 \pm 0.083$ ) compared with both the No protection ( $1.583 \pm 0.300$ ) and hAM groups ( $1.167 \pm 0.167$ ;  $p < 0.05$ ). While the difference between the No protection and hAM groups was not significant ( $p > 0.05$ ), a significant difference was observed between the hEP and hAM groups ( $p < 0.05$ ). In the distal site, Laminin B expression was lower in the hEP group ( $1.333 \pm 0.333$ ) compared with the crush site but still higher than in the hAM group ( $0.667 \pm 0.167$ ). Although the hEP group exhibited higher levels than the No protection group ( $1.500 \pm 0.289$ ), this difference did not reach statistical significance (Figure 9b).

#### 3.6.3. Confirmation of increased NGF expression at the crush repair site following hEP application

**At the 6-week follow-up**, NGF expression in the crush region was higher in the hEP group ( $0.833 \pm 0.441$ ) compared with the No protection ( $0.500 \pm 0.289$ ) and hAM groups ( $0.167 \pm 0.167$ ). However, these differences were not statistically significant ( $p > 0.05$ ). In the distal region, NGF expression was also highest in the hEP group ( $1.250 \pm 0.144$ ) compared with the hAM ( $0.750 \pm 0.144$ ) and No protection groups ( $0.833 \pm 0.333$ ), though no significant differences were observed between the groups ( $p > 0.05$ ) (Figure 8c).

**At the 12-week follow-up**, NGF levels at the crush site showed a significant increase in the hEP group compared with the No protection group ( $1.750 \pm 0.250$  vs.  $0.417 \pm 0.167$ ;  $p < 0.05$ ). While NGF expression was also higher in the hEP group compared with the hAM group ( $1.000 \pm 0.289$ ), this difference did not reach statistical significance ( $p > 0.05$ ). A notable difference was observed between the hEP and No protection groups ( $p < 0.001$ ). In the distal region, NGF levels decreased across all groups, with the hEP group maintaining the highest expression ( $0.500 \pm 0.289$ ), although the differences between the hEP, No protection ( $0.083 \pm 0.083$ ),



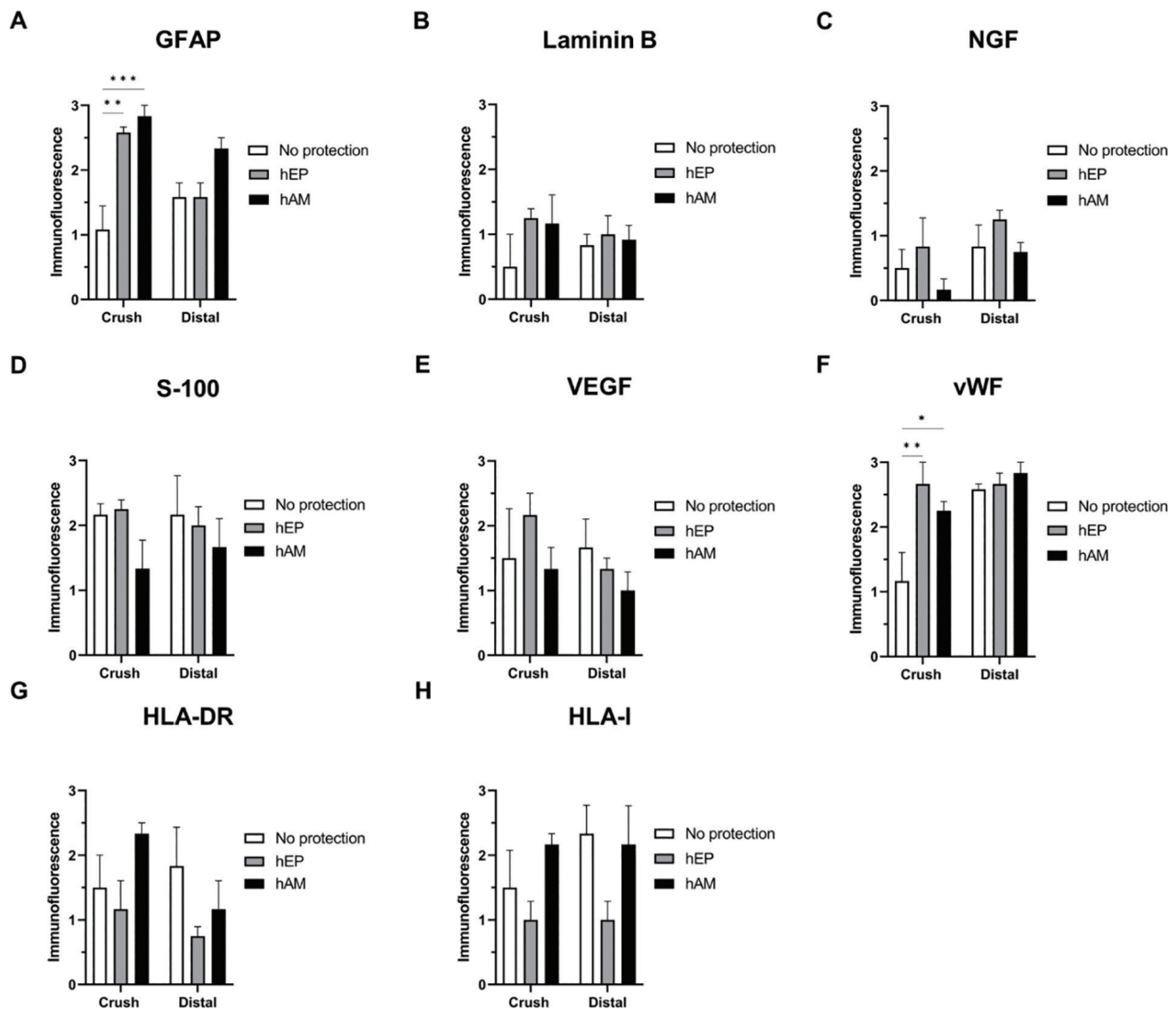


**Fig 8.** Expression evaluation of selected neurogenic, angiogenic, and immunogenic markers assessed at the crush injury sites and distal ends by immunofluorescence staining at 6 weeks following sciatic nerve crush injury, transection, and repair. (a) GFAP, (b) Laminin B, (c) NGF, (d) S-100, (e) VEGF, (f) vWF, (g) HLA-DR, and (h) HLA-I. Data were presented as mean  $\pm$  SEM. A two-way ANOVA test for group comparison was used to define statistical significance at \* $p < 0.05$ , \*\* $p < 0.01$ , \*\*\* $p < 0.001$ , and \*\*\*\* $p < 0.0001$ . GFAP, glial fibrillary acidic protein; HLA-DR, human leukocyte antigen-DR; HLA-I, human leukocyte antigen class I; NGF, nerve growth factor; SEM, standard error of the mean; VEGF, vascular endothelial growth factor; vWF, von Willebrand factor.

and hAM ( $0.167 \pm 0.167$ ) groups were not statistically significant ( $p > 0.05$ ). Despite this decrease, NGF levels in the hEP group remained elevated relative to the other groups (Figure 9c).

### 3.6.4. Confirmation of increased S-100 expression at the crush repair site following hEP application

**At the 6-week follow-up**, in the crush region, S-100 expression was slightly higher in the hEP group ( $2.250 \pm 0.144$ ) compared with both the No protection ( $2.167 \pm 0.167$ ) and

hAM groups ( $1.333 \pm 0.441$ ). Similarly, in the distal region, S-100 expression was highest in the No protection group ( $2.167 \pm 0.601$ ), followed by the hEP group ( $2.000 \pm 0.289$ ), and lower in the hAM group ( $1.667 \pm 0.441$ ). No statistically significant differences were found between these groups ( $p > 0.05$ ) (Figure 8d).

**At the 12-week follow-up**, immunofluorescence measurements of S-100 indicated significantly higher levels in the hEP group at the crush site compared with both the No protection ( $2.167 \pm 0.167$  vs.  $1.167 \pm 0.167$ ;  $p < 0.01$ ) and hAM ( $2.167 \pm 0.167$  vs.  $1.000 \pm 0.289$ ;  $p < 0.001$ ) groups.

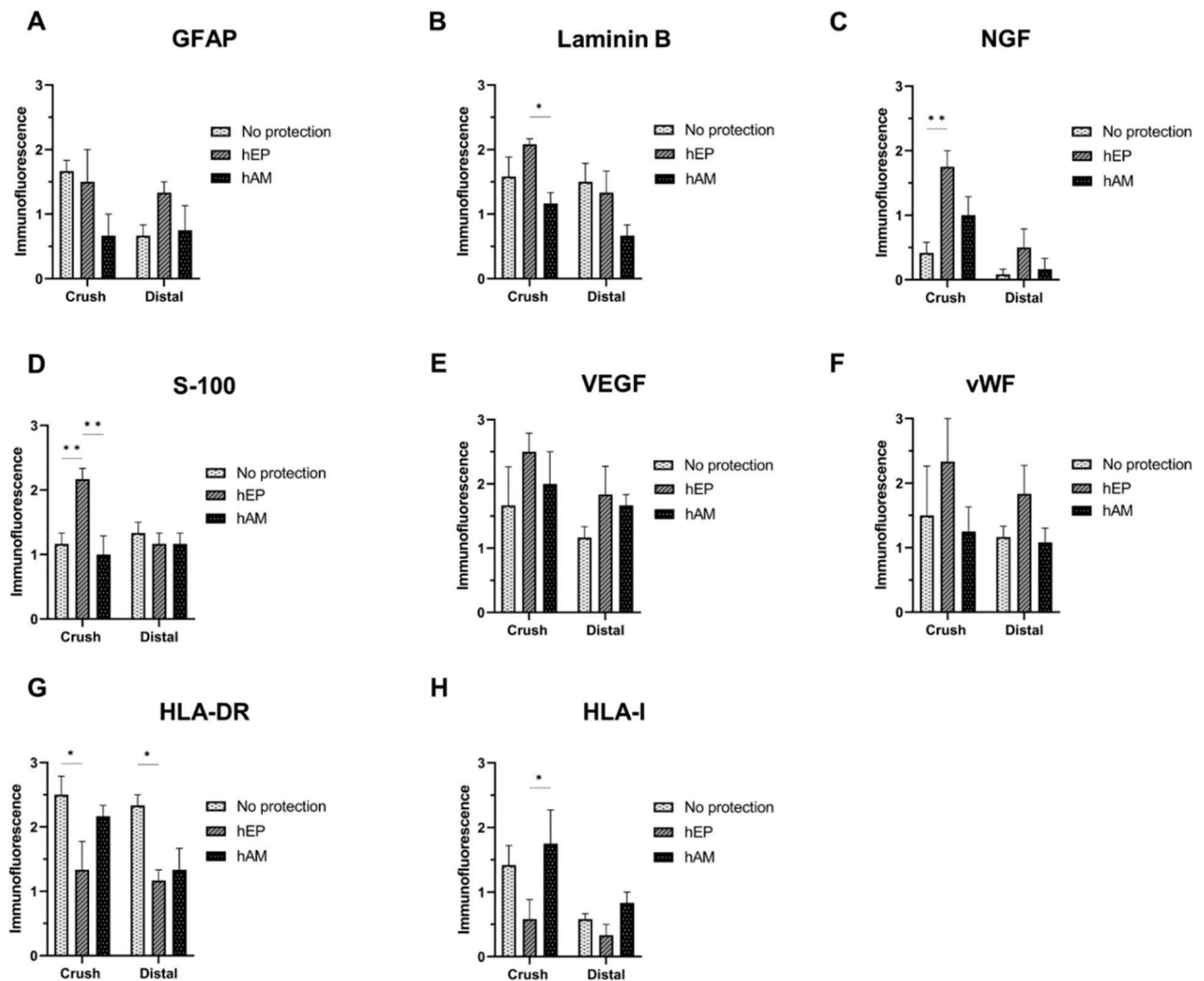


**Fig 9.** Expression evaluation of selected neurogenic, angiogenic, and immunogenic markers assessed at the crush injury sites and distal ends by immunofluorescence staining at 12 weeks following sciatic nerve crush injury, transection, and repair. (a) GFAP, (b) Laminin B, (c) NGF, (d) S-100, (e) VEGF, (f) vWF, (g) HLA-DR, and (h) HLA-I. Data were presented as mean  $\pm$  SEM. A two-way ANOVA test for group comparison was used to define statistical significance at \* $p < 0.05$ , \*\* $p < 0.01$ , \*\*\* $p < 0.001$ , and \*\*\*\* $p < 0.0001$ . GFAP, glial fibrillary acidic protein; HLA-DR, human leukocyte antigen-DR; HLA-I, human leukocyte antigen class I; NGF, nerve growth factor; SEM, standard error of the mean; VEGF, vascular endothelial growth factor; vWF, von Willebrand factor.

No significant difference was observed between the No protection and hAM groups at the crush site ( $p > 0.05$ ). At the distal site, S-100 levels were comparable across all groups, with no significant differences detected between the No protection, hEP, and hAM groups ( $p > 0.05$ ) (Figure 9d).

### 3.6.5. Confirmation of increased VEGF expression at the crush repair site following hEP application

**At the 6-week follow-up**, immunofluorescence analysis of VEGF revealed the highest levels in the hEP group at both the crush and distal sections, although no significant differences

were found between the groups. In the crush section, VEGF levels in the hEP group ( $2.500 \pm 0.289$ ) were higher than in the No protection ( $1.667 \pm 0.601$ ) and hAM groups ( $2.000 \pm 0.500$ ), but these differences did not reach statistical significance ( $p > 0.05$ ). Similarly, in the distal section, VEGF levels were elevated in the hEP group ( $1.833 \pm 0.441$ ) compared with the No protection ( $1.167 \pm 0.167$ ) and hAM ( $1.667 \pm 0.167$ ) groups, but no significant differences were detected ( $p > 0.05$ ) (Figure 8e).

**At the 12-week follow-up**, the hEP group showed significantly higher VEGF expression at the crushed site ( $2.667 \pm 0.333$ ) compared with the No protection group

( $1.167 \pm 0.441$ ) and exhibited similar values to the hAM group ( $2.833 \pm 0.167$ ). In the distal region, the hEP group ( $2.667 \pm 0.167$ ) also presented higher expression than the No protection group ( $2.583 \pm 0.083$ ) but remained close to the hAM group ( $2.833 \pm 0.167$ ). Statistical analysis revealed significant differences between the groups at the crush site ( $p < 0.01$ ) (Figure 9e).

### 3.6.6. Confirmation of increased vWF expression at the crush repair site following hEP application

**At the 6-week follow-up**, the hEP group demonstrated significantly higher vWF expression at the crush site ( $2.667 \pm 0.333$ ) than the No protection group ( $1.167 \pm 0.441$ ), achieving the most favorable results. The hEP group exhibited values similar to the hAM group ( $2.833 \pm 0.167$ ). In the distal region, the hEP group also showed elevated vWF expression ( $2.667 \pm 0.167$ ) compared with the No protection group ( $2.583 \pm 0.083$ ), with values remaining close to the hAM group ( $2.833 \pm 0.167$ ). Statistical analysis confirmed significant differences between the groups at the crush site ( $p < 0.01$ ) (Figure 8f).

**At the 12-week follow-up**, vWF immunofluorescence at the crush site revealed the highest levels in the hEP group ( $2.333 \pm 0.667$ ), compared with the No protection ( $1.500 \pm 0.764$ ) and hAM ( $1.250 \pm 0.382$ ) groups, although no statistically significant differences were detected ( $p > 0.05$ ). Similarly, at the distal site, vWF levels remained higher in the hEP group ( $1.833 \pm 0.441$ ) compared with the No protection ( $1.167 \pm 0.167$ ) and hAM ( $1.083 \pm 0.220$ ) groups, but the differences were not significant ( $p > 0.05$ ) (Figure 9f).

### 3.6.7. Confirmation of decreased HLA-DR expression following hEP application

**At the 6-week follow-up**, the hEP group exhibited lower HLA-DR expression compared with the No protection and hAM groups at both the crush site ( $1.167 \pm 0.441$  vs.  $1.500 \pm 0.500$  vs.  $2.333 \pm 0.167$ , respectively) and the distal end ( $0.750 \pm 0.144$  vs.  $1.833 \pm 0.601$  vs.  $1.167 \pm 0.441$ , respectively). Despite these differences, no significant variations were found (Figure 8g).

**At the 12-week follow-up**, immunofluorescence analysis revealed that HLA-DR levels were significantly elevated in the No protection group at both the crush ( $2.500 \pm 0.289$ ) and distal ( $2.333 \pm 0.167$ ) sites when compared with the hEP (crush:  $1.333 \pm 0.441$ ; distal:  $1.167 \pm 0.670$ ) and hAM (crush:  $2.167 \pm 0.167$ ; distal:  $1.333 \pm 0.333$ ) groups. Statistically significant differences were observed between the No protection and hEP groups at both the crush and distal sites ( $p < 0.05$ ), while other comparisons did not reach significance (Figure 9g).

### 3.6.8. Confirmation of decreased HLA-I expression at the crush repair site following hEP application

**At the 6-week follow-up**, the hEP group exhibited lower HLA-I expression compared with the No protection and hAM groups at both the crush site ( $1.000 \pm 0.289$  vs.  $1.500 \pm 0.577$  vs.  $2.167 \pm 0.167$ , respectively) and distal end ( $1.000 \pm 0.289$  vs.  $2.333 \pm 0.441$  vs.  $2.167 \pm 0.601$ , respectively). Although a significant difference was found for the column factor, no significant differences were observed in the pairwise comparisons (Figure 8h).

**At the 12-week follow-up**, HLA-I immunofluorescence levels were significantly elevated in the hAM group at the crush site ( $1.750 \pm 0.520$ ) compared with the No protection ( $1.417 \pm 0.300$ ) and hEP ( $0.583 \pm 0.300$ ) groups ( $p < 0.05$ ). However, at the distal site, no significant differences in HLA-I levels were observed among the groups, with values of  $0.583 \pm 0.083$  for No protection,  $0.333 \pm 0.167$  for hEP, and  $0.833 \pm 0.167$  for hAM (Figure 9h).

## 4. Discussion

Complex peripheral nerve injuries pose significant challenges to recovery, with outcomes varying depending on the treatment approach (Lopes et al. 2022). To address the complexities of nerve repair, well-established experimental models, such as crush or transection injuries, provide valuable clinical insights into the mechanisms of nerve regeneration (Yeoh et al. 2020). The crush injury model involves a controlled injury pattern that causes partial nerve damage while preserving overall nerve continuity. By contrast, the transection injury model results in complete nerve severance, allowing for a clear evaluation of regenerative responses following surgical repair. While various nerve repair techniques have been explored, including end-to-side coaptation with an epineurial window to facilitate axonal regeneration (Papalia et al. 2016), our study focuses on the direct application of an hEP to promote structural and functional recovery.

Although most peripheral nerve injuries in humans occur in the upper extremities, the sciatic nerve model remains the gold standard in experimental nerve regeneration research. Studies on upper limb nerves, such as the median, ulnar, and radial nerves, provide valuable alternatives, offering the benefit of faster recovery and shorter reinnervation times (Bontioti et al. 2003; Papalia et al. 2006). However, the sciatic nerve model is still preferred due to its unique advantages, including a larger diameter that enables precise surgical manipulation. Additionally, its size, length, and accessibility allow for the creation of a critical-size nerve defect, which is essential for testing various regeneration strategies (Papalia et al. 2003). These features make the sciatic nerve an effective

platform for investigating complex injury patterns and novel repair methods, which can later be translated into upper limb models for further exploration.

To better replicate the multifaceted nature of severe nerve injuries, this study introduces a novel complex sciatic nerve injury model that integrates the elements of CTR. This surgical technique promotes effective axonal regeneration and reduces the risk of secondary complications, ultimately leading to improved functional and sensory outcomes as demonstrated in our previous studies (Siemionow et al. 2002; Tetik et al. 2002).

Building on our prior findings, demonstrating that epineural conduits, grafts, sleeves, and jackets promote improved nerve regeneration while reducing inflammation and fibrosis (Lubiatowski et al. 2008; Siemionow et al. 2010, 2011, 2017a, b, 2019; Kozłowska et al. 2022; Strojny et al. 2023), we developed the hEP to enhance nerve regeneration. The hEP is characterized by low immunogenicity, negligible expression of HLA class I, and an absence of HLA class II antigens, eliminating the need for immunosuppression and making it an attractive candidate for clinical applications (Klimczak et al. 2017).

In the current study, following sciatic nerve injury and subsequent repair (CTR), we assessed the protective and regenerative potential of the hEP and compared its efficacy with a commercially available hAM (Zhang et al. 2019). Since the hEP is derived from the epineurium, the protective outermost layer of peripheral nerves, it plays a crucial role in nerve repair by facilitating cellular migration and guiding axonal regrowth. Furthermore, hEP's proangiogenic properties enhance vascularization, promoting tissue integration (Klimczak et al. 2017).

Although hAM provides anti-inflammatory and pro-regenerative benefits, its limited mechanical strength and tendency for premature degradation (Zhang et al. 2019; Ingraldi et al. 2023) may reduce its long-term efficacy, often necessitating repeat applications (Odet et al. 2021). To address these challenges, we assessed the hEP as a potentially more durable and effective solution.

Macroscopically, the hEP demonstrated stability, minimal adhesion to surrounding tissues, and limited local inflammation, creating a favorable regenerative environment. The observed vascularization around the hEP further underscores its role in facilitating nutrient delivery and waste removal. These findings align with our previous studies assessing various epineural techniques, which have shown vascularization of the epineurium derived from human donors (Tetik et al. 2002; Klimczak et al. 2017). In contrast, hAM was often not visible at the nerve repair site during follow-up evaluation. This suggests potential biodegradation or integration challenges of hAM which may impact nerve regeneration (Odet et al. 2021).

Recovery of motor and sensory function revealed significant improvement in the hEP-protected nerves compared with the hAM patch application. At earlier follow-ups, both hEP and hAM showed comparable progress in functional recovery. However, the full benefits of hEP became evident at 12 weeks, when both motor and sensory functions demonstrated optimal recovery. The progressive functional improvement observed following the hEP patch application confirms accelerated recovery of injured nerves as well as the long-term maintenance of functional restoration (Juckett et al. 2022).

Another challenge encountered after complex nerve injuries is the development of muscle atrophy, which disrupts the neural input essential for maintaining muscle integrity. Effective nerve regeneration is therefore crucial for mitigating atrophy by restoring motor function and re-establishing neural communication with the target muscles (Sulaiman and Gordon 2000). To address muscle atrophy, we assessed the GMI and found a significantly better recovery in hEP-protected nerves compared with hAM at 12 weeks post patch application. These findings suggest that the use of hEP as a protective wrap and barrier from surrounding tissues after trauma more effectively enhances both nerve regeneration and muscle mass preservation than the hAM patch effect (Lubiatowski et al. 2008).

Moreover, the observed functional improvements following the hEP patch application correlated with the histomorphometric analysis of the harvested nerve samples. This analysis demonstrated clear advantages of hEP over hAM, particularly during the later stages of nerve recovery. Interestingly, at 6 weeks, both hEP and hAM showed comparable levels of axonal density and the percentage of myelinated fibers, indicating similar early support for nerve regeneration after trauma. However, this pattern changed at the longer follow-up, favoring the hEP over hAM. At 12 weeks follow-up, hEP-protected nerves exhibited significantly increased axonal density, fiber diameters, and myelin thickness, particularly at the proximal and crushed nerve regions. This suggests sustained, enhanced, long-term remyelination and axonal regrowth. These findings underscore the superior capacity of hEP to support structural nerve recovery over time, likely due to its enhanced neuroprotective properties including structural support, myelin preservation, and the promotion of Schwann cell activity, which together facilitate more effective nerve regeneration. In contrast, while the hAM patch provided early structural benefits it lacked the sustained regenerative support observed with the hEP patch (Siemionow et al. 2022).

Finally, the advantages of the hEP patch were further validated through immunofluorescence analysis, particularly at the 12-week time-point, where a significantly more pronounced increase in the expression of Laminin B, NGF, and



S-100 markers was observed following the application of the hEP patch compared with the hAM. This finding highlights the superior neuroprotective and anti-inflammatory properties of the hEP patch, making it more effective in supporting nerve regeneration at the site of nerve injury. Additionally, at the 6-week follow-up, a significant increase in angiogenesis markers, including VEGF and vWF, was detected at the sciatic nerve crush site after hEP application, further confirming the patch's proangiogenic properties. These findings suggest the potential role of the hEP in initiating vascular remodeling during the early stages of nerve regeneration. Moreover, a similar pattern of vascular remodeling during both early and long-term stages of nerve regeneration was observed in our previous studies (Siemionow and Brzezicki 2009; Siemionow et al. 2010, 2011; Klimczak et al. 2017), further emphasizing the critical role of the hEP patch in the process of neovascularization.

It should be noted that one limitation of this study is the use of a small animal model, which may not fully replicate the complexity of human nerve injuries. Nevertheless, small animal models remain the cornerstone of experimental studies on nerve regeneration, providing a basis for comparative analysis of functional and morphological parameters. Notably, the immunodeficient rat model employed in this study enabled us to evaluate the regenerative potential of human-derived hEP and hAM products without eliciting an immune or inflammatory response. This approach was crucial for assessing the potential of hEP in nerve regeneration, highlighting its viability as a product for clinical application in humans.

In summary, we confirmed that the application of hEP at the sciatic nerve repair site following CTR injury significantly enhanced nerve regeneration compared with hAM. Moreover, the hEP patch supports long-term nerve healing through its unique features, including immunomodulatory, anti-inflammatory, and neovascularization properties, which create a protective barrier from surrounding tissues, thus facilitating the regeneration of the injured nerves. Additionally, by reducing inflammation and enhancing vascularization, hEP establishes a regenerative environment that promotes both structural repair and functional recovery.

## 5. Conclusion

This study confirmed the neuroregenerative and protective role of the hEP patch as an innovative nerve protector, demonstrating its potential to enhance nerve regeneration following complex trauma. Compared with hAM, the application of the hEP at the sciatic nerve repair site significantly improved long-term nerve regeneration, as evidenced by enhanced functional recovery. Thus, this study positions the hEP patch as a valuable addition to the armamentarium of peripheral nerve reconstructive procedures and a promising tool in the field of regenerative medicine.

## Acknowledgment

The authors thank Seiler Figuren for the technical support and staff members of Core Imaging Facilities at the University of Illinois at Chicago for embedding tissue in paraffin, mounting paraffin sections onto glass slides, and acquiring electron microscopy images. The authors acknowledge use of the BioRender software (RRID: SCR\_018361) – BioRender, Canada – Toronto, ON, Canada to create the illustrations used in this study (Figure 1).

## Funding

This research and APC were supported by the Musculoskeletal Transplant Foundation (MTF, NJ, USA), Grant #2014-06351.

## Conflict of Interest

The authors declare no conflicts of interest.

## Author Contributions

Conceptualization, MS\*; methodology, MS\*; software, WR\*, DK, LC, and GF; validation, MS\*; formal analysis, WR\*, LC, DK, and GF; investigation, KK, SB, DK, and LC; resources, MS\*; data curation, KK, SB, DK, LC, WR\*, and GF; writing – original draft preparation, WR\*, GF, and LC; writing – review and editing, MS\*; visualization, WR\* and LC; supervision, MS\*; project administration, MS\*; and funding acquisition, MS\*. All authors have read and agreed to the published version of the manuscript. \*These authors contributed equally to this work.

## Data Availability

All data generated or analyzed during this study are either included in this published article or are available from the corresponding author upon reasonable request.

## Ethical Approval

This study was approved by the Institutional Animal Care and Use Committee (IACUC) of the University of Illinois at Chicago, accredited by the AAALAC. In this study, human sciatic nerves from cadaver sources were purchased from the tissue bank, the Musculoskeletal Transplant Foundation (MTF, NJ, USA).

## Consent to Participate

All authors consent to participate.

## Consent to Publish

All authors consent to publication.

## References

- Bontioti EN, Kanje M, Dahlin LB (2003) Regeneration and functional recovery in the upper extremity of rats after various types of nerve injuries. *J Peripher Nerv Syst* 8:159–168. <https://doi.org/10.1046/j.1529-8027.2003.03023.x>
- Botelho AC, Mamede AMA, eds. (2015) Amniotic membrane: Origin, characterization, and medical applications. Springer, Berlin.
- Grinsell D, Keating CP (2014) Peripheral nerve reconstruction after injury: a review of clinical and experimental therapies. *Biomed Res Int* 2014:698256. <https://doi.org/10.1155/2014/698256>
- Gudemez E, Ozer K, Cunningham B et al. (2002) Dehydroepiandrosterone as an enhancer of functional recovery following crush injury to rat sciatic nerve. *Microsurgery* 22: 234–241. <https://doi.org/10.1002/micr.10039>
- Hussain G, Wang J, Rasul A et al. (2020) Current status of therapeutic approaches against peripheral nerve injuries: a detailed story from injury to recovery. *Int J Biol Sci* 16:116–134. <https://doi.org/10.7150/ijbs.35653>
- Ingraldi AL, Audet RG, Tabor AJ (2023) The preparation and clinical efficacy of amnion-derived membranes: a review. *J Funct Biomater* 14:531. <https://doi.org/10.3390/jfb14100531>
- Juckett L, Saffari TM, Ormseth B et al. (2022) The effect of electrical stimulation on nerve regeneration following peripheral nerve injury. *Biomolecules* 12:1856. <https://doi.org/10.3390/biom12121856>
- Klimczak A, Siemionow M, Futoma K et al. (2017) Assessment of immunologic, proangiogenic and neurogenic properties of human peripheral nerve epineurium for potential clinical application. *Histol Histopathol* 32:1197–1205. <https://doi.org/10.14670/HH-11-875>
- Kornfeld T, Vogt PM, Radtke C (2019) Nerve grafting for peripheral nerve injuries with extended defect sizes. *Wien Med Wochenschr* 169:240–251. <https://doi.org/10.1007/s10354-018-0675-6>
- Kozłowska K, RóŜczka K, Strojny MM et al. (2022) Human mesenchymal stem cells enhance nerve regeneration in nerve gap repair with human epineural conduit of a large-unmatched diameter. *J Surg* 10:193–205. <https://doi.org/10.11648/j.js.20221006.11>
- Leal-Marín S, Kern T, Hofmann N et al. (2021) Human amniotic membrane: a review on tissue engineering, application, and storage. *J Biomed Mater Res B Appl Biomater* 109:1198–1215. <https://doi.org/10.1002/jbm.b.34782>
- Lin JS, Jain SA (2023) Challenges in nerve repair and reconstruction. *Hand Clin* 39:403–415. <https://doi.org/10.1016/j.hcl.2023.05.001>
- Lopes B, Sousa P, Alvites R et al. (2022) Peripheral nerve injury treatments and advances: one Health perspective. *Int J Mol Sci* 23:918. <https://doi.org/10.3390/ijms23020918>
- Lubiatowski P, Unsal FM, Nair D et al. (2008) The epineural sleeve technique for nerve graft reconstruction enhances nerve recovery. *Microsurgery* 28:160–167. <https://doi.org/10.1002/micr.20472>
- Meng Q, Burrell JC, Zhang Q et al. (2023) Potential application of orofacial MSCs in tissue engineering nerve guidance for peripheral nerve injury repair. *Stem Cell Rev Rep* 19:2612–2631. <https://doi.org/10.1007/s12015-023-10609-y>
- Odét S, Louvrier A, Meyer C et al. (2021) Surgical application of human amniotic membrane and amnion-chorion membrane in the oral cavity and efficacy evaluation: corollary with ophthalmological and wound healing experiences. *Front Bioeng Biotechnol* 9:685128. <https://doi.org/10.3389/fbioe.2021.685128>
- Papalia I, Magaúdda L, Righi M et al. (2016) Epineurial window is more efficient in attracting axons than simple coaptation in a sutureless (cyanoacrylate-bound) model of end-to-side nerve repair in the rat upper limb: functional and morphometric evidences and review of the literature. *PLoS One* 11:e0148443. <https://doi.org/10.1371/journal.pone.0148443>
- Papalia I, Tos P, Scevola A et al. (2006) The ulnar test: a method for the quantitative functional assessment of posttraumatic ulnar nerve recovery in the rat. *J Neurosci Methods* 154:198–203. <https://doi.org/10.1016/j.jneumeth.2005.12.012>
- Papalia I, Tos P, Stagno d'Alcontres F et al. (2003) On the use of the grasping test in the rat median nerve model: a re-appraisal of its efficacy for quantitative assessment of motor function recovery. *J Neurosci Methods* 127:43–47. [https://doi.org/10.1016/s0165-0270\(03\)00098-0](https://doi.org/10.1016/s0165-0270(03)00098-0)
- Siemionow M, Bobkiewicz A, Cwykiel J et al. (2017a) Epineural sheath jacket as a new surgical technique for neuroma prevention in the rat sciatic nerve model. *Ann Plast Surg* 79:377–384. <https://doi.org/10.1097/SAP.0000000000001117>
- Siemionow M, Uygur S, Madajka M (2017b) Application of epineural sheath as a novel approach for fat volume maintenance. *Ann Plast Surg* 79:606–612. <https://doi.org/10.1097/SAP.0000000000001176>
- Siemionow M, Brzezicki G (2009) Chapter 8: current techniques and concepts in peripheral nerve repair. *Int Rev Neurobiol* 87: 141–172. [https://doi.org/10.1016/S0074-7742\(09\)87008-6](https://doi.org/10.1016/S0074-7742(09)87008-6)
- Siemionow M, Cwykiel J, Uygur S et al. (2019) Application of epineural sheath conduit for restoration of 6-cm long nerve defects in a sheep median nerve model. *Microsurgery* 39:332–339. <https://doi.org/10.1002/micr.30393>
- Siemionow M, Demir Y, Mukherjee AL (2010) Repair of peripheral nerve defects with epineural sheath grafts. *Ann Plast Surg* 65:546–554. <https://doi.org/10.1097/SAP.0b013e3181fd6b18>
- Siemionow M, Duggan W, Brzezicki G et al. (2011) Peripheral nerve defect repair with epineural tubes supported with bone marrow stromal cells: a preliminary report. *Ann Plast Surg* 67:73–84. <https://doi.org/10.1097/SAP.0b013e318223c2db>
- Siemionow M, Strojny MM, Kozłowska K et al. (2022) Application of human epineural conduit supported with human mesenchymal stem cells as a novel therapy for enhancement of nerve gap regeneration. *Stem Cell Rev Rep* 18:642–659. <https://doi.org/10.1007/s12015-021-10301-z>
- Siemionow M, Tetik C, Ozer K et al. (2002) Epineural sleeve neurorrhaphy: surgical technique and functional results – a

- preliminary report. *Ann Plast Surg* 48:281–285. <https://doi.org/10.1097/00000637-200203000-00009>
- Siemionow M, Uygur S, Ozturk C et al. (2013) Techniques and materials for enhancement of peripheral nerve regeneration: a literature review. *Microsurgery* 33:318–328. <https://doi.org/10.1002/micr.22104>
- Strojny MM, Kozłowska K, Brodowska S et al. (2023) Assessment of human epineural conduit of different size diameters on efficacy of nerve regeneration and functional outcomes. *J Reconstr Microsurg* 39:392–404. <https://doi.org/10.1055/s-0042-1758182>
- Sulaiman OA, Gordon T (2000) Effects of short- and long-term Schwann cell denervation on peripheral nerve regeneration, myelination, and size. *Glia* 32:234–246. [https://doi.org/10.1002/1098-1136\(200012\)32:3<234::aid-glia40>3.0.co;2-3](https://doi.org/10.1002/1098-1136(200012)32:3<234::aid-glia40>3.0.co;2-3)
- Tetik C, Ozer K, Ayhan S et al. (2002) Conventional versus epineural sleeve neurorrhaphy technique: functional and histomorphometric analysis. *Ann Plast Surg* 49:397–403. <https://doi.org/10.1097/00000637-200210000-00011>
- Thakker A, Sharma SC, Hussain NM et al. (2021) Nerve wrapping for recurrent compression neuropathy: a systematic review. *J Plast Reconstr Aesthet Surg* 74:549–559. <https://doi.org/10.1016/j.bjps.2020.10.085>
- Thomson SE, Ng NY, Riehle MO et al. (2022) Bioengineered nerve conduits and wraps for peripheral nerve repair of the upper limb. *Cochrane Database Syst Rev* 12:CD012574. <https://doi.org/10.1002/14651858.CD012574.pub2>
- Wang ML, Rivlin M, Graham JG et al. (2019) Peripheral nerve injury, scarring, and recovery. *Connect Tissue Res* 60:3–9. <https://doi.org/10.1080/03008207.2018.1489381>
- Yeoh S, Warner WS, Eli I et al. (2020) Rapid-stretch injury to peripheral nerves: comparison of injury models. *J Neurosurg* 135:893–903. <https://doi.org/10.3171/2020.5.JNS193448>
- Zhang ZY, Yang J, Fan ZH et al. (2019) Fresh human amniotic membrane effectively promotes the repair of injured common peroneal nerve. *Neural Regen Res* 14:2199–2208. <https://doi.org/10.4103/1673-5374.262596>